Structures in the energy dependence of classical and quantum bremsstrahlung

A. Florescu†‡, O. I. Obolensky†¶, C. D. Shaffer§, and R. H. Pratt†

† *Department of Physics and Astronomy, University of Pittsburgh, Pittsburgh, PA 15260, USA*
‡ *Institute for Space Science, Bucharest, Romania*
¶ *The A.F. Ioffe Physico-Technical Institute, St. Petersburgh 194021, Russia*
§ *Department of Mathematics and Computer Science, Westminster College, New Wilmington, PA, USA*

Abstract. A study of the origin of structures in the energy dependence of electron bremsstrahlung is presented. There is a similarity between classical and quantum results. In the quantum case a connection between zeroes of dipole matrix elements and structures in the bremsstrahlung cross section and asymmetry parameter is established. In the classical case it is found that classical trapping, which results in a singular behavior of the scattering angle with impact parameter, is not directly responsible for the observed structures.

INTRODUCTION

We present here a study of the origin of structures in the energy dependence of the electron bremsstrahlung cross section $\frac{k\mathrm{d}\sigma}{\mathrm{d}k}$ and the asymmetry parameter a_2 for a given ratio of photon energy k and projectile electron energy T. The asymmetry parameter characterizes the angular distribution of radiation:

$$\frac{k\,\mathrm{d}^2\sigma}{\mathrm{d}k\,\mathrm{d}\Omega_k} = \frac{1}{4\pi}\frac{k\mathrm{d}\sigma}{\mathrm{d}k}\left(1+\frac{a_2}{2}P_2(\cos\theta_k)\right), \qquad (1)$$

where Ω_k is the photon emission angle and P_2 is the Legendre polinomial.

We illustrate the structures for the case of an Al atom in Fig. 1 (for calculations performed in a quantum approach) and in Fig. 2 (for a classical approach). The structures were first seen in numerical calculations of angular distributions of electron bremsstrahlung in a screened atomic potential for Al within the framework of classical electrodynamics (1). Similar features were later observed in the corresponding quantum case for Eu (2). Here we show our quantum results for Al, which are qualitatively similar to the classical results. We have subsequently also seen similar structures in the energy dependence of the classical cross section (3), see Figs. 1 and 2. The correspondence between classical and quantum structures encourages the belief that they are real physical phenomena. (However modifications due to classical (4) or quantum (5) polarizational bremstrahlung from the atomic structure have not yet been examined.)

It had initially been noted (1) that in the classical case these structures were developing as the electron en-

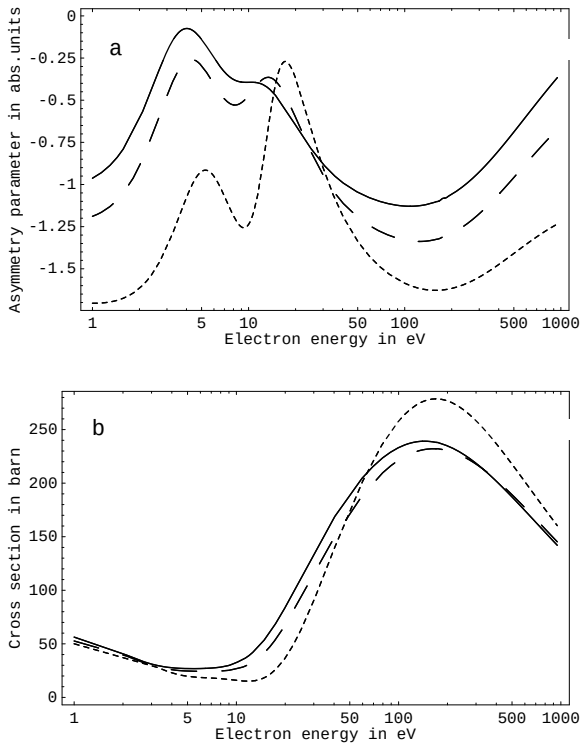

FIGURE 1. Quantum case: energy dependence of (a) the asymmetry parameter a_2 and (b) the cross section, for Al for different ratios of photon energy k and projectile electron energy T: solid line $k/T = 0.01$, dashed line $k/T = 0.2$, dotted line $k/T = 0.6$.

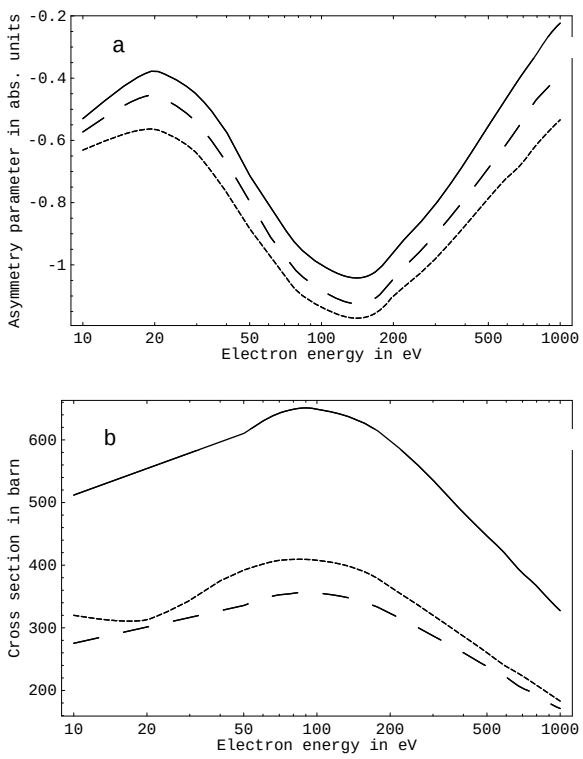

FIGURE 2. Classical case: energy dependence of (a) the asymmetry parameter a_2 and (b) the cross section, for Al for different ratios of photon energy k and projectile electron energy T: solid line $k/T = 0$, dashed line $k/T = 0.2$, dotted line $k/T = 0.4$.

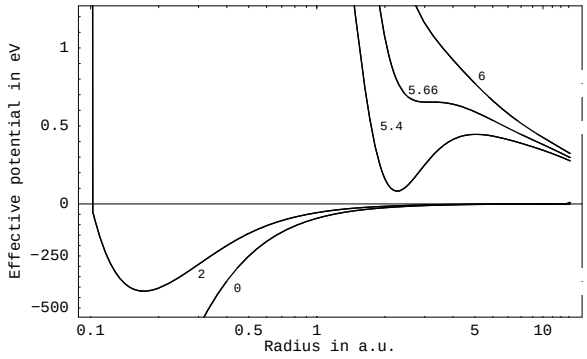

FIGURE 3. Effective potentials $V_{\rm eff}$ in Al for different values of Λ (see Eq. 2). The effective potential has an inflection point at $\Lambda = \Lambda_{\rm M} = 5.66$ with a corresponding energy $T_{\rm M} = 0.64$ eV. Note different scales for negative and positive values of the effective potential.

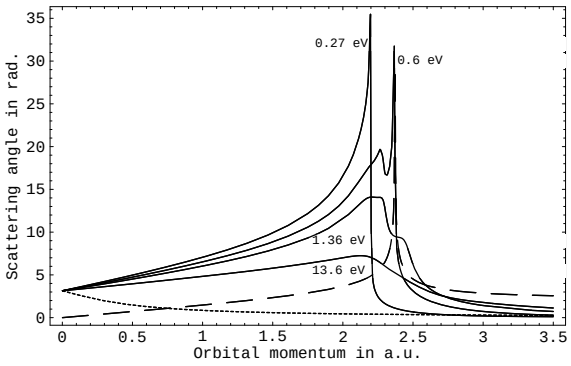

FIGURE 4. Scattering angle $\phi(T,L)$ as a function of L for several values of energy T (solid lines). Dashed line corresponds to Eq. 5, dotted line corresponds to the Coulomb point field.

ergy approached the maximum energy of classical trapping from above. Classical trapping occurs in a screened Coulomb potential when the projectile electron energy (at given angular momentum L) is equal to the height of the barrier in the effective potential

$$V_{\rm eff}(L,r) = V(r) + \Lambda/(2mr^2), \qquad (2)$$

where $V(r)$ is the atomic potential, m is the projectile mass, $\Lambda = L(L+1)$ in the quantum case and $\Lambda = L^2$ in the classical case. (Effective potentials for various values of Λ are plotted in Fig. 3.) For such a trajectory the radial component of acceleration vanishes at the turning point of radial motion, and the incoming electron is trapped by the target. (The corresponding quantum phenomena is the presence of shape resonances in scattering.) For nearby energies and nearby angular momenta the electron will make many revolutions about the target before escaping. Thus, in a screened potential, the scattering angle $\phi(T,L)$, considered as a function of electron energy T and momentum L, has a singularity, changing fast for nearby energies and momenta, as shown in Fig. 4. At a certain value $\Lambda = \Lambda_{\rm M}$ the effective potential has an inflection point (with a corresponding energy $T = T_{\rm M}$) and then the outer barrier coalesces with the centrifugal barrier. For Al $\Lambda_{\rm M} = 5.66$ and $T_{\rm M} = 0.64$ eV. Trapping is not possible at energies higher than $T_{\rm M}$. Since there is no outer barrier in the point Coulomb potential there is no trapping in the Coulomb case, and the scattering angle is a smooth function of L and T.

It had been supposed (1) that the classical structures were connected to the onset of trapping. Our present studies show that, to the contrary, the observed structures are not directly associated with the trapping or the resonances: The near-singular region of classical scattering does not contribute to the cross sections. Shape resonances do not affect the quantum asymmetry parameter (in fact resonances are not present at these energies), but the structures are rather associated with the presence of zeroes in dominant matrix elements. (Of course there are connections among these phenomena, just as the number

of zeroes in a matrix element is connected with the number of bound states in a potential (6).)

In the next two sections we will describe the classical and then the quantum approaches, particularly focusing on the soft photon limit situation, simpler to describe and already illustrating the structure features.

CLASSICAL DESCRIPTION

A classical approach may be used for the description of bremsstrahlung processes at low projectile energies, both in the point Coulomb potential (7) and in screened atomic potentials (1, 3, 8). The motion of a beam of projectiles in the scattering potential is calculated in the frame of classical mechanics, and classical electrodynamics is used to obtain the radiation on electron orbits and the resulting radiation spectrum. Analytic results are available in the point Coulomb field case, for both the spectrum (9) and for the asymmetry parameter (7); both have been tabulated (7). Numerical results, as illustrated in Fig. 2, have been obtained for screened potentials (1, 3), obtaining structures (oscillations) which are not present in the Coulomb case. (In (1) the structures in the spectrum had not been observed because, as discussed in (3), the spectra were plotted with a scaling factor T/Z^2 which masked the behavior.)

We see from Fig. 2 that the main features of the structures are already present in the soft photon limit case, for which the description and procedure of calculation may be simplified. In this case the expressions for the spectrum and asymmetry parameter may be written as (we use the atomic system $e = \hbar = m = 1$)

$$\frac{k\,\mathrm{d}\sigma}{\mathrm{d}k} = \frac{8}{3c^3}\int_0^\infty L\,\mathrm{d}L(1-\cos\phi(T,L)), \qquad (3)$$

$$a_2 = \frac{\int_0^\infty L\,\mathrm{d}L(1-\cos\phi(T,L))(3\cos\phi(T,L)-1)}{\int_0^\infty L\,\mathrm{d}L(1-\cos\phi(T,L))}. \qquad (4)$$

For energies near the maximum trapping energy T_M a singular behavior develops in L, as illustrated in Fig. 4. We have been able to obtain an expression for this behavior by making an expansion of $\phi(T,L)$ in Taylor series about the point (T_M, $L_\mathrm{M} = \sqrt{\Lambda_\mathrm{M}}$)

$$\phi(T,L) \sim \left\{\frac{\gamma}{2}\left[\frac{6}{\gamma}\left(\delta T - \frac{\delta L\, L_\mathrm{M}}{m r_0^2}\right)\right]^{\frac{2}{3}} + \frac{2\delta L\, L_\mathrm{M}}{m r_0^3}\right\}^{-\frac{1}{2}}, \qquad (5)$$

where $\delta T \equiv T - T_\mathrm{M}$, $\delta L \equiv L - L_\mathrm{M}$, r_0 is the inflection point in $V_\mathrm{eff}(L_\mathrm{M}, r)$, and

$$\gamma = -\left.\frac{\partial^3 V_\mathrm{eff}(L,r)}{\partial r^3}\right|_{r=r_0,\,L=L_M}.$$

This expression well characterizes the singular behavior of the scattering angle and also the right wing of the peak, but it soon fails in the left wing (see Fig.).

One might suppose that this singular behavior is responsible for the observed structures or oscillations in the spectrum and asymmetry parameter. However, in fact, a singular behavior in $\phi(T,L)$ leads to rapid oscillations of the trigonometric functions of Eqs. 3,4, so that such a region does not contribute in the integration over impact parameters. One can see this analytically. (This result is contrary to the suggestion in (1) that oscillation in ϕ is unlikely to be averaged by the integration.)

Thus we conclude that the trapping singularity which occurs in screened potentials is not directly responsible for the observed oscillations.

QUANTUM DESCRIPTION

Our calculations indicate that the structures seen in classical bremsstrahlung are also can be found in the quantum case (Fig. 1). The similarity is only qualitative.

In a quantum calculation one obtains the spectrum and asymmetry parameter by summing contributions of dipole transition radial matrix elements of low initial and final angular momentum. The expressions for the spectrum is (2)

$$\frac{k\,\mathrm{d}\sigma}{\mathrm{d}k} = 16\pi^2\frac{ck^4}{T}\sum_{l_1,l_2} l_> |<\nu_2||r||\nu_1>|^2, \qquad (6)$$

where l_1 and l_2 are the orbital momenta of the projectile electron in initial and final states, $l_> = \max(l_1, l_2)$, $<\nu_2||r||\nu_1>$ is the dipole matrix element between states $|\nu_1>$ and $<\nu_2|$. Quantum expression for the asymmetry parameter is rather complicated and we do not write it here.

Magnitudes of the terms in Eq. 6, which give the main contribution to the total cross section are shown in Fig. 5. The main features can again be understood from the soft photon case, on which we will now focus.

It is evident that within this formalism the structures in the spectrum (and similarly in the asymmetry parameter) are to be understood as resulting from zeroes in dominant radial matrix elements. In the spectrum at low energy the transition matrix elements $0 \to 1$ and $1 \to 0$ are dominant; we are denoting the matrix elements by the initial and final orbital momenta of the projectile electron. These then decrease to have zeroes, resulting in a minimum.

Note, that in the soft photon limit, $k/T \to 0$, matrix elements $0 \to 1$ and $1 \to 0$, $1 \to 2$ and $2 \to 1$ and so on are equal, while for larger k/T the behaviors of the pairs of matrix elements are more spread out, resulting in less pronounced structures. Comparing results for different k/T,

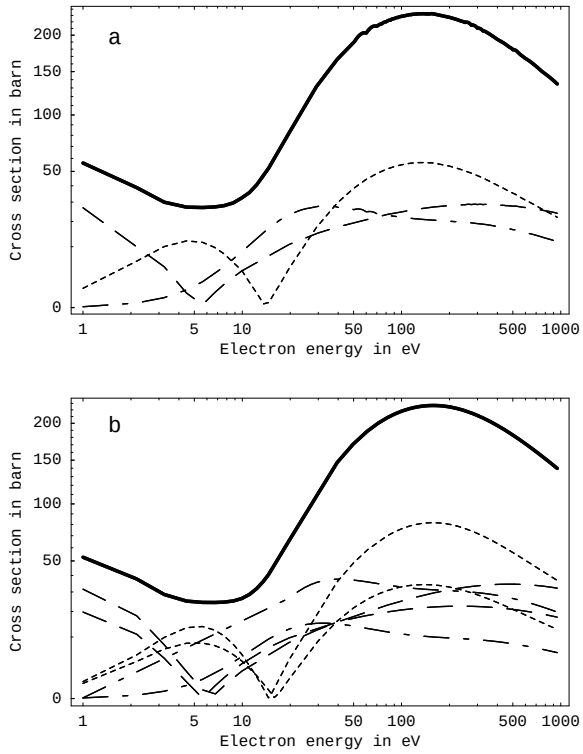

FIGURE 5. Partial contributions of dominant matrix elements to the total bremsstrahlung cross section (thick solid line) for the two values of ratio k/T: 0.01 (a) and 0.2 (b). Dashed lines correspond to $0 \to 1$ and $1 \to 0$ transitions, dotted lines correspond to $1 \to 2$ and $2 \to 1$ transitions and dashed-dotted lines correspond to $2 \to 3$ and $3 \to 2$ transitions. Note that for the soft photon limit $k/T \to 0$ matrix elements $\ell \to \ell'$ and $\ell' \to \ell$ are equal. For finite value of k/T the matrix elements are spread out; we do not label them separately here. Note also that positions of matrix elements zeroes depends on photon energy k.

one can also see that the positions of zeroes in matrix elements vary with the energies of the initial and final states; the trajectories of the positions of matrix element zeroes have been discussed in (6). Note also that from this viewpoint we would not expect further structures at still lower energies, unless the transition $0 \leftrightarrow 1$ had further zeroes – which it should not, based on our other work (6). This had not been clear in the numerical classical calculations, which failed for energies too near the maximum trapping energy $T_{\rm M}$.

We see that the classical and quantum structures are qualitatively similar. Perhaps this reflects a connection between classical trapping and quantum bound states and resonances. It is known that there is a connection between numbers of bound states and numbers of matrix element zeroes (6). Evidently further study is needed.

ACKNOWLEDGMENTS

This work is supported by NSF grant 9970293 and by the Russian Foundation for Basic Research under the grant 99-02-18294-a.

REFERENCES

1. Kim, L., and Pratt, R. H., *Phys. Rev. A* **36**, 45-58 (1987).
2. Korol, A. V., Lyalin, A. G., and Solovyov, A. V., *J. Phys. B: At.Mol.Opt.Phys.* **28**, 4947-4962 (1995).
3. Shaffer, C. D., *Issues in Electron-Atom Bremsstrahlung*, Ph.D. thesis, University of Pittsburgh, Pittsburgh (1996).
4. Kogan, V. I., and Kukushkin, A. B., *Sov. Phys. — JETP* **60**, 665-675 (1984).
5. *Polarization Radiation*, edited by V. N. Tsitovich and I. M. Oiringel, Plenum, New York, 1993
6. Shaffer, C. D., Pratt, R. H., and Oh, S. D., *Phys. Rev. A* **56**, 3653-3658 (1997).
7. Florescu, V., and Costescu, A., *Rev. Roum. Phys.* **23**, 131 (1978).
8. Astapenko, V. A., Bureeva, L. A., and Lisitsa, V. S., *JETP* **90**, 434-446 (2000).
9. Kramers, H. A., *Phil. Mag.* **46**, 836-871 (1923).